

# Striatal Dopamine Deficit and Motor Impairment in Idiopathic Normal Pressure Hydrocephalus

Nicoló Gabriele Pozzi, MD,<sup>1,2</sup> Joachim Brumberg, MD,<sup>3</sup>  Massimiliano Todisco, MD,<sup>1,4\*</sup>  Brigida Minafra, MD,<sup>1</sup> Roberta Zangaglia, MD,<sup>1</sup> Irene Bossert, MD, PhD,<sup>5</sup> Giuseppe Trifirò, MD,<sup>5</sup> Roberto Ceravolo, MD,<sup>6</sup>  Paolo Vitali, MD, PhD,<sup>7</sup> Ioannis Ugo Isaias, MD, PhD,<sup>2</sup> Alfonso Fasano, MD, PhD,<sup>8,9,10,11</sup>  and Claudio Pacchetti, MD<sup>1</sup>

<sup>1</sup>Parkinson's Disease and Movement Disorders Unit, IRCCS Mondino Foundation, Pavia, Italy

<sup>2</sup>Neurology Department, University Hospital and Julius Maximilian University of Würzburg, Würzburg, Germany

<sup>3</sup>Nuclear Medicine Department, University Hospital Würzburg, Würzburg, Germany

<sup>4</sup>Department of Brain and Behavioral Sciences, University of Pavia, Pavia, Italy

<sup>5</sup>Nuclear Medicine Unit, Istituti Clinici Scientifici Maugeri SpA SB IRCCS, Pavia, Italy

<sup>6</sup>Unit of Neurology, Department of Clinical and Experimental Medicine, University of Pisa, Pisa, Italy

<sup>7</sup>Neuroradiology Unit, IRCCS Mondino Foundation, Pavia, Italy

<sup>8</sup>Edmond J. Safra Program in Parkinson's Disease, Morton and Gloria Shulman Movement Disorders Clinic, Toronto Western Hospital, University Health Network, Toronto, Ontario, Canada

<sup>9</sup>Division of Neurology, University of Toronto, Toronto, Ontario, Canada

<sup>10</sup>Krembil Brain Institute, Toronto, Ontario, Canada

<sup>11</sup>CenteR for Advancing Neurotechnological Innovation to Application (CRANIA), Toronto, Ontario, Canada

**ABSTRACT: Background:** Idiopathic normal pressure hydrocephalus can present with parkinsonism. However, abnormalities of the striatal dopamine reuptake transporter are unclear.

**Objectives:** To explore presence and features of striatal dopaminergic deficit in subjects with idiopathic normal pressure hydrocephalus as compared to Parkinson's disease (PD) patients and healthy controls.

**Methods:** We investigated 50 subjects with idiopathic normal pressure hydrocephalus, 25 with PD, and 40 healthy controls. All participants underwent [<sup>123</sup>I]-N-ω-fluoropropyl-2β-carbomethoxy-3β-(4-iodophenyl)nortropine and single-photon emission computed tomography to quantify the striatal dopamine reuptake transporter binding. All subjects with idiopathic normal pressure hydrocephalus underwent a levodopa (L-dopa) challenge test and magnetic resonance imaging to evaluate ventriculomegaly and white matter changes. Gait, cognition, balance, and continence were assessed with the Idiopathic Normal Pressure Hydrocephalus Rating Scale, and parkinsonism with the motor section of the Movement Disorder Society-Unified Parkinson's Disease Rating Scale. All patients completed a 2-year follow-up.

**Results:** A total of 62% of patients with idiopathic normal pressure hydrocephalus featured a reduced striatal dopamine reuptake transporter binding, which correlated with the severity of parkinsonism but not with features of ventriculomegaly or white matter changes. Unlike PD, this dopaminergic deficit in idiopathic normal pressure hydrocephalus was more symmetric and prominent in the caudate nucleus.

**Conclusions:** Subjects with idiopathic normal pressure hydrocephalus can present a reduction of striatal dopamine reuptake transporter binding, which is consistent with the severity of parkinsonism and qualitatively differs from that found in PD patients. Longitudinal interventional studies are needed to prove a role for striatal dopamine reuptake transporter deficit in the pathophysiology of idiopathic normal pressure hydrocephalus. © 2020 International Parkinson and Movement Disorder Society

**Key Words:** idiopathic normal pressure hydrocephalus; SPECT; striatal dopamine; parkinsonism; Parkinson's disease

\*Correspondence to: Massimiliano Todisco. Parkinson's Disease and Movement Disorders Unit, IRCCS Mondino Foundation. Via Mondino 2, 27100, Pavia, Italy. Tel: +39 0382 380221; Fax +39 0382 380226; E-mail: massimiliano.todisco@mondino.it

**Relevant conflicts of interests/financial disclosures:** Nothing to report.

**Funding agencies:** This study was approved and funded by Italian Ministry of Health and co-funded by Health-Service of Lombardy (project code number RF-2013-02355908: "Idiopathic Normal Pressure

Hydrocephalus (iNPH), parkinsonism and dementia: improving the accuracy of diagnosis and the patient care to reverse the symptomatology. Neurodegeneration, phenotypes and outcome measures").

**Received:** 30 May 2020; **Revised:** 24 September 2020; **Accepted:** 30 September 2020

**Published online in Wiley Online Library**  
(wileyonlinelibrary.com). DOI: 10.1002/mds.28366

## Introduction

Idiopathic normal pressure hydrocephalus (iNPH) is a neurological disease that affects up to 3% of subjects over 65 years.<sup>1,2</sup> It is characterized by progressive locomotor, cognitive, and urinary disturbances, but its onset can be very heterogeneous, and it often mimics other neurodegenerative diseases, thus causing misdiagnosis and treatment delays.<sup>2–5</sup> In particular, up to 71% of subjects with iNPH can present parkinsonian features.<sup>2,3,6</sup> Because many patients have balance and locomotor difficulties (ie, slowness, shuffling steps, freezing of gait, en bloc turns, and impaired balance with falls), gait impairment of iNPH can closely resemble the features of Parkinson's disease (PD) and it is often classified as “higher-level gait disorder” (HLGD).<sup>4,7</sup> Additionally, more than 60% of iNPH patients show bradykinesia and asymmetric symptoms at onset.<sup>2,3</sup> The reasons of this clinical resemblance are largely unknown, but recent molecular imaging findings suggested a role for the striatal dysfunction in iNPH pathophysiology.<sup>8</sup>

Molecular imaging of presynaptic nigrostriatal neurons with [<sup>123</sup>I]-N- $\omega$ -fluoropropyl-2 $\beta$ -carbomethoxy-3 $\beta$ -(4-iodophenyl)nortropine (FP-CIT) and single-photon emission computed tomography (SPECT) consistently shows abnormalities of dopamine reuptake transporter (DAT) binding in PD patients and correlates with disease severity.<sup>9</sup> Instead, in iNPH DAT changes remain unclear and range from normal to pathological findings in up to 46% of the subjects.<sup>10–12</sup>

Here, we investigated the striatal DAT binding with FP-CIT SPECT in subjects with iNPH as compared to PD patients and healthy controls (HC). We also assessed the correlation between striatal FP-CIT binding and motor impairment in iNPH patients and explored the relationship between SPECT findings and magnetic resonance imaging (MRI) features of ventriculomegaly and white matter abnormalities.

## Methods

### Study Design

Between January 2016 and March 2018, as a first cross-sectional part of a larger prospective study, we evaluated clinical and molecular imaging findings of patients with iNPH and PD, recruited at the “Parkinson's Disease and Movement Disorders Unit” of the IRCCS Mondino Foundation in Pavia (Italy). In particular, we explored FP-CIT SPECT differences among 50 subjects with iNPH, 25 with newly diagnosed PD, and 40 age-matched HC. Controls were individuals who had no neurological symptom and a normal neurological examination. Patients performed FP-CIT SPECT on average 3 months after the clinical and MRI assessment. After molecular imaging, iNPH

patients were treated with levodopa (L-dopa) 600 mg daily (200 mg t.i.d.) for at least 3 months followed by an acute challenge test with L-dopa 250 mg. The significant improvement with L-dopa was established as at least 30% reduction in the motor section of the Movement Disorder Society-sponsored revision of the Unified Parkinson's Disease Rating Scale (MDS-UPDRS III).<sup>13,14</sup> Study population was followed up for at least 2 years.

### Clinical and MRI Assessment

All patients were clinically evaluated by a movement disorder specialist and underwent an MRI protocol with a 3T MRI scanner (32-channel head coil, Siemens Skyra, Syngo MR D13C version, Erlangen, Germany). We acquired diffusion-weighted imaging (DWI), FLAIR, dual echo proton density (PD)-T<sub>2</sub>, and T<sub>2</sub>\* sequences in axial planes, covering the whole brain. We also obtained a three-dimensional T<sub>1</sub> MPRAGE sequence (TR = 2300, TE = 2.95, TI = 900, 270 sagittal slices with no gap, voxel size: 1.1 × 1.1 × 1.2, acquisition time: 5'15"). The local Institutional Review Board approved the study and all participants gave written informed consent.

Probable iNPH was diagnosed according to the International Guidelines.<sup>15</sup> In particular, the diagnosis of iNPH was confirmed by Evans' index >0.30 and at least 1 of the following supportive features at MRI<sup>15,16</sup>: acute callosal angle on reformatted coronal T<sub>1</sub>-weighted images at the level of the posterior commissure (perpendicular to the anterior commissure–posterior commissure plane); aqueductal or fourth ventricular flow void on PD-T<sub>2</sub>-weighted sagittal images; and disproportionately enlarged subarachnoid space hydrocephalus (DESH) (ie, obliteration of the high-convexity sulci on reformatted axial T<sub>1</sub>-weighted images and dilation of the Sylvian fissures on reformatted coronal T<sub>1</sub>-weighted images). We performed a qualitative assessment of the callosal angle, which was defined as acute when lower than 90° as in the original study.<sup>17</sup> We also evaluated periventricular and deep white matter hyperintensities on axial FLAIR images with the Fazekas scale.<sup>18</sup>

We excluded causes of secondary hydrocephalus (ie, positive history of head trauma, intracerebral hemorrhage, meningitis) as well as other neurological, psychiatric (ie, major depression), or general medical conditions explaining the clinical presentation. In addition, neurological examination of subjects with iNPH did not show any red flag sign suggestive of atypical parkinsonism.

A tap test (ie, large volume lumbar puncture) removing at least 40 mL of cerebrospinal fluid (CSF) was performed, also to ascertain that the CSF opening pressure was within the 70–245 mmH<sub>2</sub>O range.<sup>15</sup> A positive

response was defined as at least 10% improvement of 10-meter seconds or steps 5 hours after the tap test.<sup>19</sup> Subjects with a negative response to the tap test (14 patients) underwent an external lumbar drainage lasting 4 days and removing 100–150 mL of CSF per day. They all had a positive response as defined earlier.<sup>19</sup>

In iNPH patients, gait, cognition, balance, and continence were evaluated with the iNPH Rating Scale.<sup>20</sup> We also considered 2 gait patterns of iNPH as previously described<sup>7</sup>: a disequilibrium subtype of HLGD (phenotype 1) (ie, wide base and externally rotated feet) and a locomotor subtype of HLGD (phenotype 2) (ie, normal base, start hesitation, freezing of gait, shuffling steps, and en bloc turning).

Subjects with PD were diagnosed according to the Movement Disorder Society criteria.<sup>21</sup> In all patients with either PD or iNPH, the severity of parkinsonian signs was assessed by means of the MDS-UPDRS III,<sup>13</sup> and cognition with education-adjusted scores of the Mini Mental State Examination (MMSE).<sup>22</sup>

A surgical CSF diversion was offered to all patients, and 12 subjects declined in favor of a “wait and see” approach given their mild impairment of activities of daily living and/or fear of surgery. All iNPH patients who underwent surgery had a sustained improvement of their condition; these subjects have been included in a recently published trial detailing shunt outcome.<sup>19</sup>

### Molecular Imaging

All patients (PD and iNPH) and HC underwent SPECT with FP-CIT to measure striatal DAT binding. All subjects with iNPH were tested before eventual surgical intervention. Scans were acquired 180 minutes after injection of  $182.4 \pm 3.6$  MBq of FP-CIT on a dual-headed SPECT system (Infinia, GE Healthcare, Eindhoven, Netherlands) equipped with a fan-beam collimator (step-and-shoot mode, 1 frame/4°/45 seconds, photopeak window of  $159 \text{ keV} \pm 15\%$ , matrix  $128 \times 128$ ). Reconstruction was performed on a Xeleris platform (GE Healthcare) with filtered back projection pre-filtering with Butterworth cut-off of 0.55 cycles/cm and order 10.

### Image Analysis

All image data were processed and analyzed using the relevant toolboxes of PMOD image analysis software version 4.0 (PMOD Technologies Ltd, Zurich, Switzerland). Semiquantitative evaluation of SPECT data was applied to calculate the specific binding ratio (SBR) of FP-CIT as a direct measure of count concentration in striatal volumes of interest (VOI). Individuals’ SPECT data were normalized to a dedicated FP-CIT SPECT template in the standard anatomical space of the Montreal Neurological Institute (MNI).<sup>23,24</sup> Based on the Automated Anatomic Labeling Atlas

(AAL),<sup>25</sup> VOI were defined comprising paired VOI for caudate nucleus, putamen, and whole striatum, and large bilateral occipital lobe VOI. After the delineation of the VOI on the normalized data, VOI-based partial volume correction was performed with PMOD considering a spatial resolution of 12 mm at full width at half maximum (FWHM).<sup>26,27</sup> Finally, we calculated the average regional uptake values in the VOI and SBR for caudate nucleus, putamen, and striatum for both hemispheres using the occipital cortex as reference region:<sup>28</sup>

$$\left( \frac{\text{average counts per voxel VOI}}{\text{average counts per voxel VOI OCCIPITAL}} \right) - 1. \quad (1)$$

Due to partial volume effect and its possibly insufficient correction when using tight striatal VOI, we confirmed the results of SBR with a second quantification procedure (ie, the Southampton method), which is based on the specific uptake size index (SUSI) in the striatum.<sup>29</sup> For this analysis, summed striatal images were created for each individual, containing the slice with the hottest striatal voxel and 5 slices on either side. In a second step, a region of interest (ROI) of standard shape and large dimensions was manually placed around the left and the right striatum on the two-dimensional summed striatal images. Furthermore, we defined a standardized reference ROI, which incorporated the whole brain in the summed image except for the striatal regions. Of note, large striatal VOI may also involve low count rates from nearby gray and white matter or CSF. However, possible group differences between subjects with iNPH, PD patients, and HC would also apply for background VOI, and thus we considered this effect negligible. The striatal binding ratios were calculated assuming a striatal volume of 11.4 mL as previously described<sup>29,30</sup>:

$$\left( \frac{\text{background subtracted total counts ROI STRIATUM}}{\text{Volume STRIATUM}} \right) \times \text{count concentration ROI REFERENCE}. \quad (2)$$

### Outcome Measures and Statistical Analysis

Demographic and clinical data were tested with *t* or  $\chi^2$  test as appropriate.

Concerning molecular imaging, we first evaluated how many iNPH and PD patients showed a pathological reduction of striatal DAT binding. In this regard, we defined a reference range by computing the mean SBR of HC for striatum, caudate, and putamen of both hemispheres and considering  $\pm 2$  SD as upper and lower limits for normal DAT binding. We computed the

number of subjects with iNPH and PD showing pathological SBR reductions in the more depleted striatum (ie, falling outside this reference range) and for the caudate and putamen values separately.

We then compared SBR values of iNPH and PD patients with HC for caudate nucleus and putamen, separately. We ensured the normal distribution of the data in each group and then performed a 2-tailed ANOVA, corrected for multiple comparisons with Dunnett's test.

To assess the lateralization of SBR changes, we computed the asymmetry index (AI) as previously described:<sup>29,30</sup>

$$\frac{(SBR_{STRIATUMMORE} - SBR_{STRIATUMLESS})}{(SBR_{STRIATUMMORE} + SBR_{STRIATUMLESS})} \times 200, \quad (3)$$

where MORE and LESS refer to the striatum with the higher and lower SBR values with respect to the contralateral hemisphere, respectively.<sup>31,32</sup> A *t* test was used to compare AI between iNPH and PD groups.

To analyze whether subjects with iNPH and PD showed a distinctive reduction of striatal uptake, we also calculated the caudate/putamen ratio (C/P ratio) as:

$$\frac{SBR_{CAUDATELESS}}{SBR_{PUTAMENIPSI}}, \quad (4)$$

where LESS refers to the caudate with the lowest SBR value and IPSI to the putamen of the same hemisphere. We then tested whether the C/P ratio could differentiate iNPH from PD by means of a logistic regression analysis, where the diagnosis (iNPH vs. PD) was the dependent variable, and the C/P ratio was the independent variable. We used a receiver operating characteristic (ROC) analysis to identify the optimal cut-off value.

We also investigated the correlation between SBR of caudate nucleus and putamen, and the severity of parkinsonian signs as measured with the MDS-UPDRS III score in subjects with iNPH and PD. Finally, in iNPH patients we explored the correlation between striatal SBR values, symptoms evaluated with iNPHRS scores, response to tap test, and MRI features of ventriculomegaly and white matter abnormalities. With this regard, we performed a multivariate analysis and computed Spearman's  $\rho$ . For all analyses, we considered  $P < 0.05$  as significant.

Statistical analyses were performed by means of JMP statistical package, version 13 (SAS Institute, Cary, NC).

## Results

Demographic, clinical, MRI, and SPECT features of the recruited subjects are shown in Table 1. Patients

and HC did not differ with respect to gender and age. Subjects with iNPH and PD were also similar in terms of MDS-UPDRS III, whereas MMSE scores were lower in iNPH patients (vs. PD:  $P < 0.05$ ; vs. HC:  $P < 0.01$ ). Because we recruited only subjects with newly diagnosed PD, the 2 patients groups differed with regard to disease duration ( $P < 0.01$ ).

Seventeen (34%) subjects with iNPH featured a phenotype 1, whereas 33 (66%) showed a phenotype 2. MDS-UPDRS III score was higher in iNPH patients with phenotype 2 as compared to those with phenotype 1 ( $22.3 \pm 8.3$  vs.  $8.4 \pm 5.1$ , respectively:  $P < 0.001$ ). Similar differences were found in bradykinesia ( $9.5 \pm 6.2$  vs.  $3.1 \pm 2.2$ :  $P < 0.001$ ), rigidity ( $3.3 \pm 2.1$  vs.  $0$ :  $P < 0.001$ ), and axial scores ( $8.1 \pm 2.4$  vs.  $3.8 \pm 1.9$ :  $P < 0.001$ ).

All subjects with PD showed a marked improvement with dopaminergic treatment. In contrast, no iNPH patient significantly responded to L-dopa, neither after chronic treatment nor after acute challenge test. No patient's diagnosis was converted into atypical parkinsonism during the 2-year follow-up period.

### SPECT Findings across Groups

With respect to the reference range of HC, 31 (62%) subjects with iNPH showed a pathological decrease of striatal DAT binding, when considering the most affected hemisphere. The number of iNPH patients with reduction of SBR values increased to 37 (74%) when taking into account only the most affected caudate nucleus and decreased to 26 (52%) when considering only the most affected putamen (Fig. 1). The FP-CIT binding of striatum and putamen of the most affected side was pathological in all subjects with PD. SBR values of the most affected caudate nucleus were reduced in 10 (40%) PD patients. No age-related difference between groups was identified with respect to striatal, putamen, and caudate SBR values. For further comparisons, only the most affected hemisphere was considered.

We found that striatal SBR values were similar between subjects with iNPH (entire cohort, including both phenotypes) and PD ( $2.7 \pm 0.4$  in both groups) and reduced in both cohorts when compared to HC ( $3.4 \pm 0.3$ :  $P < 0.05$ ). In particular, the average caudate binding of subjects with iNPH was lower than that of PD patients ( $2.6 \pm 0.4$  vs.  $2.8 \pm 0.4$ , respectively:  $P < 0.05$ ) and both groups differed from HC ( $3.4 \pm 0.3$ :  $P < 0.01$ ) (Fig. 2). The average putaminal SBR values were instead lower in subjects with PD than iNPH patients ( $2.4 \pm 0.3$  vs.  $2.8 \pm 0.5$ , respectively:  $P < 0.05$ ) and—again—both differed from HC ( $3.4 \pm 0.4$ :  $P < 0.01$ ) (Fig. 2). The lateralization of the SBR reduction differed between iNPH and PD, showing a greater AI in PD as compared to iNPH ( $6.5 \pm 3.6$  vs.  $2.7 \pm 1.8$ , respectively:  $P < 0.01$ ). The C/P ratio also

**TABLE 1.** Demographic, clinical, MRI, and SPECT features of the sample

	iNPH (n = 50)	PD (n = 25)	HC (n = 40)
Gender (male/female)	26/24	13/12	18/22
Age at FP-CIT SPECT (years)	74.4 ± 4.5	71.0 ± 5.6	73.0 ± 4.5
Disease duration (years)	2.7 ± 1.1	1.3 ± 0.4	–
MMSE (score)	24.2 ± 3.1	26.8 ± 5.4	28.2 ± 1.6
MDS-UPDRS III (score)	18.1 ± 14.0	17.1 ± 8.0	–
iNPHRS gait (score)	62.9 ± 18.5	–	–
iNPHRS neuropsychology (score)	87.5 ± 9.5	–	–
iNPHRS balance (score)	66.4 ± 17.3	–	–
iNPHRS continence (score)	84.9 ± 8.7	–	–
iNPHRS total (score)	72.9 ± 16.6	–	–
Evans' index	0.37 ± 0.04	–	–
Acute callosal angle	37 (74.0)	–	–
Flow void	21 (42.0)	–	–
DESH	42 (84.0)	–	–
Fazekas scale for PWM (score)	2.2 ± 0.9	–	–
Fazekas scale for DWM (score)	1.6 ± 0.7	–	–
More affected striatum SBR	2.73 ± 0.42	2.55 ± 0.31	3.42 ± 0.32
More affected striatum SUSI SBR	3.63 ± 1.05	3.20 ± 0.89	5.78 ± 0.88

Abbreviations: DESH, disproportionately enlarged subarachnoid space hydrocephalus; DWM, deep white matter; FP-CIT SPECT, single-photon emission computed tomography with [<sup>123</sup>I]-N-ω-fluoropropyl-2β-carbomethoxy-3β-(4-iodophenyl)nortropine; HC, healthy controls; iNPH, idiopathic normal pressure hydrocephalus; iNPHRS, iNPH Rating Scale; MDS-UPDRS III, Movement Disorder Society-sponsored revision of the Unified Parkinson's Disease Rating Scale, motor section; MMSE, Mini Mental State Examination; PD, Parkinson's disease; PWM, periventricular white matter; SBR, specific binding ratio; SUSI, specific uptake size index.

Data are shown as number of patients (%) or mean ± SD. Disease duration was calculated from the onset of motor symptoms to the age at FP-CIT SPECT.

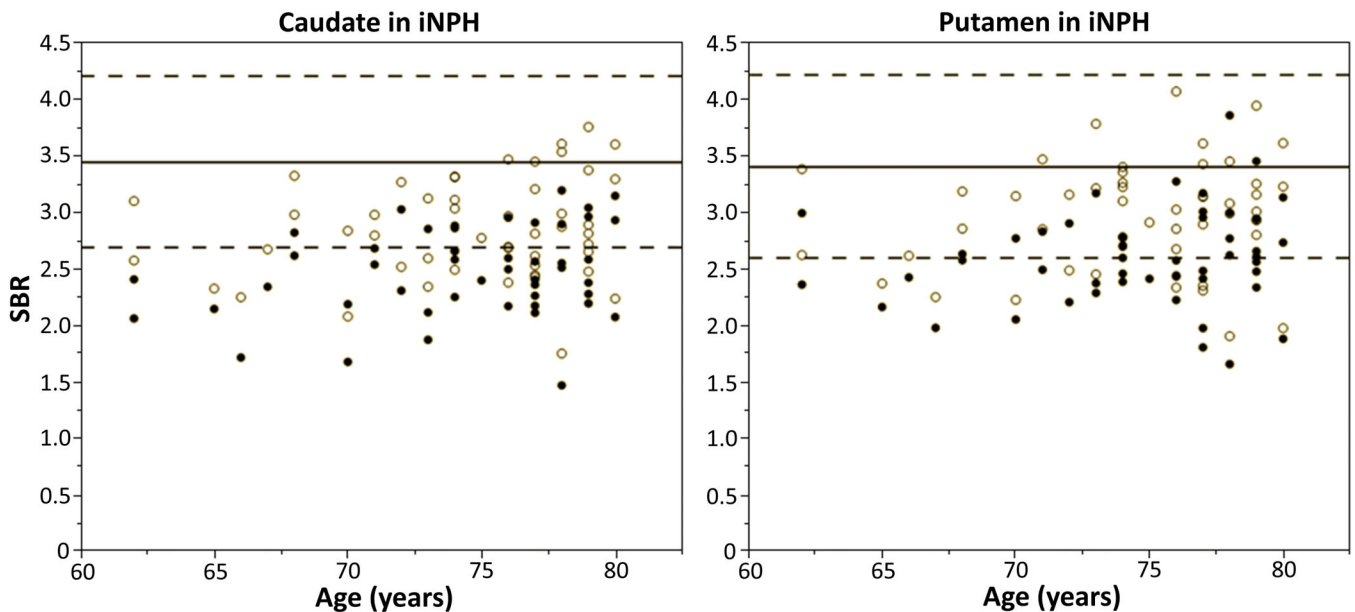


**FIG. 1.** Individual caudate and putamen DAT binding values of iNPH patients with respect to HC. The individual DAT binding (SBR value) for caudate nucleus and putamen of all iNPH patients is reported. Black and white dots refer to the more and less affected sides, respectively. The mean values and reference (normative) intervals ( $\pm 2$  SD) of HC are reported as full and dashed lines, respectively. Values falling below this interval were considered pathological. DAT, dopamine reuptake transporter; HC, healthy controls; iNPH, idiopathic normal pressure hydrocephalus; SBR, specific binding ratio.

differed between iNPH and PD ( $0.83 \pm 0.12$  vs.  $1.09 \pm 0.14$ ;  $P < 0.01$ ), and the value of 0.94 distinguished iNPH from PD with specificity of 90% and sensitivity of 86.7% (logistic regression,  $R^2 = 0.45$ ,  $P < 0.01$ ) (Fig. 3). In particular, a reduction of C/P ratio of 0.1 was associated with an odds ratio of 3.80 (95%

confidence interval = 2.14–6.75) for the diagnosis of iNPH.

When exploring the between-phenotype differences within the iNPH group, striatal SBR values were found lower than HC in 5 of 17 (29.4%) iNPH patients with phenotype 1 and in 26 of 33 (78.8%) iNPH patients

with phenotype 2 ( $P < 0.01$ ). The average of putamen SBR values ( $2.3 \pm 0.2$  vs.  $2.6 \pm 0.2$ ;  $P < 0.01$ ) and caudate SBR values ( $2.7 \pm 0.4$  vs.  $3.0 \pm 0.3$ ;  $P < 0.01$ ) were lower in phenotype 2 than phenotype 1.

### Correlation Analysis of SPECT Findings

In the iNPH group, we did not detect any correlation of FP-CIT binding of putamen and caudate nucleus with disease duration. In PD patients, DAT binding of putamen, but not of caudate nucleus, inversely correlated with disease duration ( $\rho = -0.18$ ,  $P = 0.03$ ).

In subjects with iNPH (entire cohort), we found an inverse correlation between the MDS-UPDRS III score and SBR values for the caudate nucleus ( $\rho = -0.25$ ,  $P = 0.01$ ) and the putamen ( $\rho = -0.26$ ,  $P = 0.008$ ) (Fig. 4). The correlation was also detected when considering iNPH patients with phenotype 2, both for the caudate nucleus ( $\rho = -0.28$ ,  $P = 0.005$ ) and the putamen ( $\rho = -0.30$ ,  $P = 0.003$ ). In PD patients, we found an inverse correlation ( $\rho = -0.56$ ,  $P = 0.004$ ) between the MDS-UPDRS III score and SBR values of the most affected putamen, whereas no correlation was identified with caudate SBR values.

Finally, we did not show any correlation of DAT binding of putamen and caudate nucleus with domains of the iNPH Rating Scale, response to tap test, or MRI features of ventriculomegaly and white matter changes (ie, Evans' index, acute callosal angle, DESH, and Fazekas scale).

## Discussion

In this study, we found that iNPH patients can present reduced striatal DAT binding as compared to HC and a pattern of DAT reduction different from that of

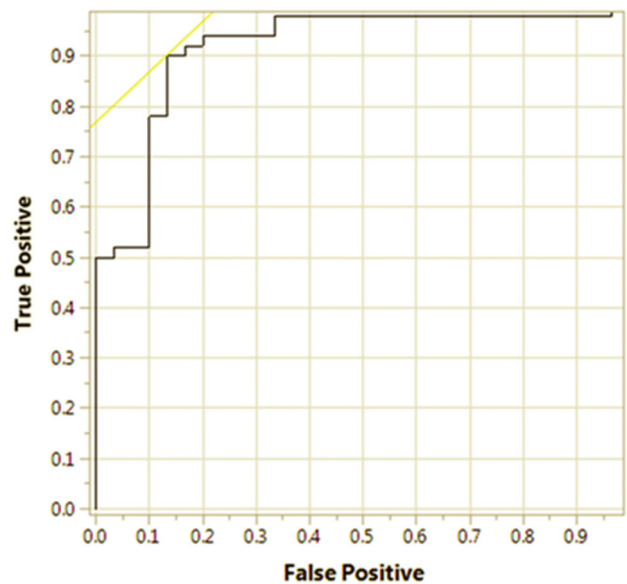


**FIG. 3.** ROC analysis of the caudate/putamen ratio. The ROC curve of the logistic regression of SBR values of the most affected side predicting diagnosis between PD and iNPH is reported. We used iNPH as positive level. The area under the curve equals to 91.7%. iNPH, idiopathic normal pressure hydrocephalus; PD, Parkinson's disease; ROC, receiver operating characteristic; SBR, specific binding ratio.

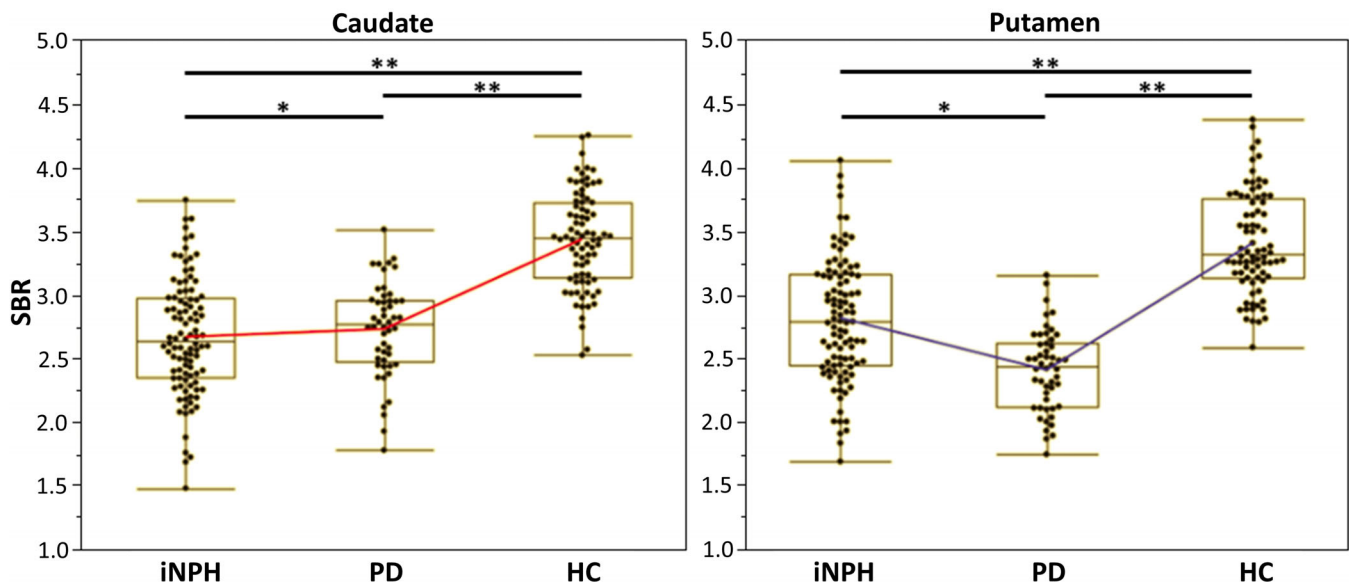


**FIG. 2.** DAT binding reduction in iNPH, PD, and HC. The box-plots show the different DAT binding (SBR value) in caudate nucleus and putamen of the most affected hemisphere for iNPH and PD as well as for HC. For each group the single values (dots), the mean values, and the 95% confidence intervals (box-plots) are reported. For sake of comparison between groups, caudate mean DAT densities are connected by a red line, and putamen mean values are connected by a blue line. Horizontal bars denote significant differences ( $*P < 0.05$ ,  $**P < 0.01$ ). DAT, dopamine reuptake transporter; PD, Parkinson's disease; HC, healthy controls; iNPH, idiopathic normal pressure hydrocephalus; SBR, specific binding ratio.

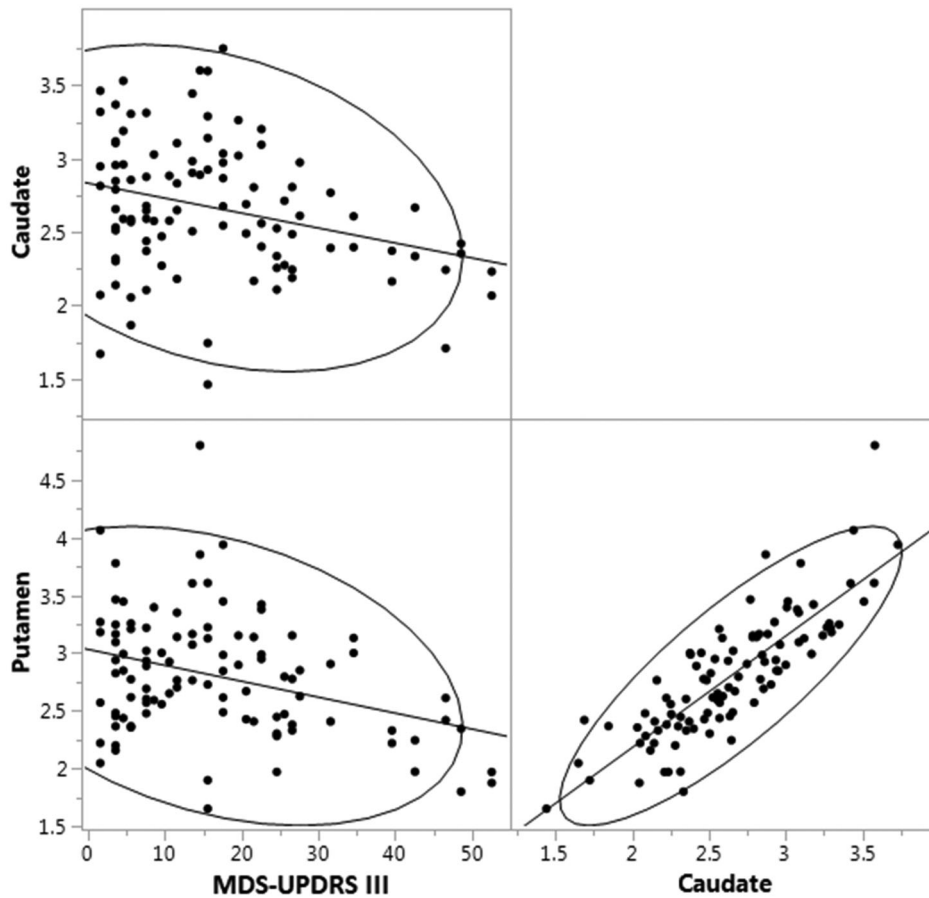


**FIG. 4.** Correlation of MDS-UPDRS III with caudate and putamen DAT binding in iNPH. The scatterplot matrix shows the inverse correlation between caudate DAT values and severity of the motor impairment as assessed with the MDS-UPDRS III. Ellipsoids represent the 95% confidence intervals. Putamen DAT values also show an inverse correlation with MDS-UPDRS III scores. Caudate and putamen DAT values instead show a direct correlation. DAT binding of the most affected hemisphere is reported. DAT, dopamine reuptake transporter; iNPH, idiopathic normal pressure hydrocephalus; MDS-UPDRS III, Movement Disorder Society-sponsored revision of the Unified Parkinson’s Disease Rating Scale, motor section.

PD. Unlike the consistent, lateralized, and mainly putaminal DAT loss displayed by PD patients, the reduction of DAT binding in subjects with iNPH was mainly present in patients with the locomotor subtype and—when impaired—it was more symmetric and prominent in the caudate nucleus. Accordingly, the computation of the C/P ratio distinguished the two conditions with specificity of 90% and sensitivity of 86.7% (Fig. 3). Moreover, we showed a correlation between striatal DAT loss and motor impairment evaluated with the MDS-UPDRS III, without any correlation with motor and non-motor domains of the iNPH Rating Scale or MRI features. The correlation was driven by the group of patients with more prominent gait involvement (ie, phenotype 2).

Few studies investigated the DAT loss in subjects with iNPH and reported inconsistent results.<sup>10–12</sup> Hence, the relevance of FP-CIT SPECT in iNPH is still questioned. Ouchi et al.<sup>11</sup> assessed 8 iNPH patients and described a preserved presynaptic activity in the nigrostriatal dopaminergic system that was associated with a reduction of postsynaptic D2 receptors, thus suggesting a prominent

striatal alteration in iNPH. On the contrary, DAT deficit in iNPH was reported by 2 studies.<sup>10,12</sup> In particular, Broggi et al.<sup>10</sup> found a striatal DAT loss in 47% and Allali et al.<sup>12</sup> in 31% of subjects with iNPH. These studies did not categorize patients on the basis of the type of motor impairment (balance vs. locomotion). Furthermore, and in contrast with these studies, we highlighted the DAT deficit of caudate nucleus as an important feature in iNPH, particularly if compared to the prominent putaminal loss in PD. In fact, these 2 previous studies did not take into account a partial volume effect as possible methodological drawback of acquisition and analysis of SPECT scans.

Studies in animal models of iNPH reported a concomitant impairment of locomotor performances and nigrostriatal dopaminergic activity as measured by means of tyrosine hydroxylase immunoreactivity assays.<sup>33,34</sup> Our results in subjects with iNPH support these preliminary findings in animal models of iNPH and suggest that an impairment of dopaminergic system may be associated with parkinsonism in iNPH. Recent MRI studies in iNPH promoted the hypothesis of a

direct structural damage of the striatum due to ventricles enlargement.<sup>35,36</sup> These authors indeed reported diminished volume of caudate nucleus in iNPH patients<sup>35</sup> and abnormal diffusion tensor imaging metrics in the posterior limb of the internal capsule, improving after shunt surgery.<sup>36</sup> The role of dopaminergic deficit at the caudate level is supported by existing literature<sup>37</sup>: a study with dopaminergic positron emission tomography (PET) showed evidence of more prominent (predominantly right) caudate nucleus denervation in PD patients with freezing of gait,<sup>38</sup> also in keeping with dopaminergic PET studies in patients receiving fetal graft implants, which have linked gait improvement with the restoration of dopaminergic transmission in the caudate nucleus.<sup>39,40</sup>

The idea that striatal DAT loss may be directly induced by structural distortion of nigrostriatal fibers caused by altered CSF dynamics is tempting, but DAT deficits in iNPH may also rely on an independent neurodegenerative process.<sup>3,41-43</sup> Alternatively, these 2 mechanisms may co-exist and interact with each other.<sup>44</sup> Direct assessments of DAT binding changes after pharmacological and surgical treatments are needed to unveil the mechanism of DAT reduction in iNPH, which remain currently unclear.<sup>3,4</sup> With this aim, longitudinal evaluations are ongoing in our center.

Our study presents some limitations, and the findings should be interpreted with caution. First, we cannot rule out a ROI misplacement. We normalized SPECT images to the MNI template using the PMOD spatial normalization routine, but an uptake bias cannot be excluded given the anatomical distortions in iNPH. Moreover, the partial volume effect might enlarge this bias by altering striatal VOI count concentration of subjects with morphologic brain changes.<sup>11,30,45</sup> We accounted for these issues by using 2 quantification methods<sup>26,29</sup> with distinctive approaches to both partial volume loss and morphologic irregularities, and we obtained congruent findings (ie, strong linear correlation of binding ratios and consistent differences of binding values between groups). Still, because both the whole brain and the large striatal ROI also include ventricular spaces, this additional analysis cannot completely rule out a ROI misplacement bias. Second, we analyzed the ventriculomegaly according to conventional MRI features (eg, Evans' index) and did not perform an automated volumetry, thus we cannot exclude a correlation between DAT binding and this accurate MRI parameter. Third, the diagnosis of probable iNPH was performed relatively soon after disease onset on clinical grounds, in absence of brain pathology. However, all the criteria of the current guidelines were fulfilled, and we also conducted a follow-up for at least 2 years in all subjects, thus minimizing the possibility of phenoconversion into atypical parkinsonisms or other mimics. In addition, all shunted patients had a

sustained improvement, in keeping with a recent proposal of characterizing iNPH diagnosis on the basis of shunt response.<sup>43</sup>

In conclusion, our data provide evidence for an impairment of the nigrostriatal dopaminergic system in iNPH with a characteristic pattern of predominant DAT deficit symmetrically involving the caudate nucleus. Prospective studies are needed to disentangle the mechanism of these alterations and fully elucidate their role in the disease. Moreover, a co-registration of SPECT and MRI images will be needed to overcome the possible bias of ROI misplacement and to confirm our findings. With these advancements, it will be possible to better address whether the DAT deficit in iNPH can be reversed with shunt surgery, thus paralleling the clinical improvement of iNPH patients, a research question currently investigated in our centre. ■

## References

1. Jaraj D, Rabiei K, Marlow T, et al. Prevalence of idiopathic normal-pressure hydrocephalus. *Neurology* 2014;82:1449-1454.
2. Krauss JK, Regel JP, Droste DW, et al. Movement disorders in adult hydrocephalus. *Mov Disord* 1997;12:53-60.
3. Morishita T, Foote KD, Okun MS. INPH and Parkinson disease: differentiation by levodopa response. *Nat Rev Neurol* 2010;6:52-56.
4. Williams MA, Malm J. Diagnosis and treatment of idiopathic normal pressure hydrocephalus. *Continuum (Minneapolis)* 2016;22:579-599.
5. Picascia M, Pozzi NG, Todisco M, et al. Cognitive disorders in normal pressure hydrocephalus with initial parkinsonism in comparison with de novo Parkinson's disease. *Eur J Neurol* 2019;26:74-79.
6. Todisco M, Pozzi NG, Zangaglia R, et al. Pisa syndrome in idiopathic normal pressure hydrocephalus. *Parkinsonism Relat Disord* 2019;66:40-44.
7. Nutt JG. Higher-level gait disorders: an open frontier. *Mov Disord* 2013;28:1560-1565.
8. Townley RA, Botha H, Graff-Radford J, et al. <sup>18</sup>F-FDG PET-CT pattern in idiopathic normal pressure hydrocephalus. *NeuroImage Clin* 2018;18:897-902.
9. Tatsch K, Poepperl G. Nigrostriatal dopamine terminal imaging with dopamine transporter SPECT: an update. *J Nucl Med* 2013;54:1331-1338.
10. Broggi M, Redaelli V, Tringali G, et al. Normal pressure hydrocephalus and parkinsonism: preliminary data on neurosurgical and neurological treatment. *World Neurosurg* 2016;90:348-356.
11. Ouchi Y, Nakayama T, Kanno T, et al. In vivo presynaptic and postsynaptic striatal dopamine functions in idiopathic normal pressure hydrocephalus. *J Cereb Blood Flow Metab* 2007;27:803-810.
12. Allali G, Garibotto V, Mainta IC, et al. Dopaminergic imaging separates normal pressure hydrocephalus from its mimics. *J Neurol* 2018;265:2434-2441.
13. Goetz CG, Tilley BC, Shaftman SR, et al. Movement Disorder Society-sponsored revision of the unified Parkinson's disease rating scale (MDS-UPDRS): scale presentation and clinimetric testing results. *Mov Disord* 2008;23:2129-2170.
14. Merello M, Nouzeilles MI, Arce GP, Leiguarda R. Accuracy of acute levodopa challenge for clinical prediction of sustained long-term levodopa response as a major criterion for idiopathic Parkinson's disease diagnosis. *Mov Disord* 2002;17:795-798.
15. Relkin N, Marmarou A, Klinge P, et al. INPH guidelines, part II: diagnosing idiopathic normal-pressure hydrocephalus. *Neurosurgery* 2005;57:4-16.

16. Mori E, Ishikawa M, Kato T, et al. Guidelines for management of idiopathic normal pressure hydrocephalus: second edition. *Neurol Med Chir* 2012;52:775–809.
17. Ishii K, Kanda T, Harada A, et al. Clinical impact of the callosal angle in the diagnosis of idiopathic normal pressure hydrocephalus. *Eur Radiol* 2008;18:2678–2683.
18. Fazekas F, Chawluk JB, Alavi A, et al. MR signal abnormalities at 1.5 T in Alzheimer’s dementia and normal aging. *AJR Am J Roentgenol* 1987;149:351–356.
19. Todisco M, Picascia M, Pisano P, et al. Lumboperitoneal shunt in idiopathic normal pressure hydrocephalus: a prospective controlled study. *J Neurol* 2020;267:2556–2566.
20. Hellström P, Klinge P, Tans J, Wikkelsø C. A new scale for assessment of severity and outcome in iNPH. *Acta Neurol Scand* 2012; 126:229–237.
21. Postuma RB, Berg D, Stern M, et al. MDS clinical diagnostic criteria for Parkinson’s disease. *Mov Disord* 2015;30:1591–1601.
22. Folstein MF, Folstein SE, McHugh PR. “Mini-mental state”. A practical method for grading the cognitive state of patients for the clinician. *J Psychiatr Res* 1975;12:189–198.
23. García-Gómez FJ, García-Solís D, Luis-Simón FJ, et al. Elaboration of the SPM template for the standardization of SPECT images with 123I-Ioflupane. *Rev Esp Med Nucl Imagen Mol* 2013;32:350–356.
24. Ashburner J, Friston KJ. Nonlinear spatial normalization using basis functions. *Hum Brain Mapp* 1999;7:254–266.
25. Tzourio-Mazoyer N, Landeau B, Papathanassiou D, et al. Automated anatomical labeling of activations in SPM using a macroscopic anatomical parcellation of the MNI MRI single-subject brain. *Neuroimage* 2002;15:273–289.
26. Rousset OG, Ma Y, Evans AC. Correction for partial volume effects in PET: principle and validation. *J Nucl Med* 1998;39:904–911.
27. Morita K, Maebatake A, Iwasaki R, et al. Evaluation of the reconstruction parameters of brain dopamine transporter SPECT images obtained by a fan beam collimator: a comparison with parallel-hole collimators. *Asia Ocean J Nucl Med Biol* 2018;6:120–128.
28. Innis RB, Cunningham VJ, Delforge J, et al. Consensus nomenclature for in vivo imaging of reversibly binding radioligands. *J Cereb Blood Flow Metab* 2007;27:1533–1539.
29. Tossici-Bolt L, Hoffmann SMA, Kemp PM, et al. Quantification of [123I]FP-CIT SPECT brain images: an accurate technique for measurement of the specific binding ratio. *Eur J Nucl Med Mol Imaging* 2006;33:1491–1499.
30. Tossici-Bolt L, Dickson JC, Sera T, et al. [123I]FP-CIT ENC-DAT normal database: the impact of the reconstruction and quantification methods. *EJNMMI Phys* 2017;4:8.
31. Arnulfo G, Pozzi NG, Palmisano C, et al. Phase matters: a role for the subthalamic network during gait. *PLoS One* 2018;13:e0198691.
32. Isaias IU, Benti R, Goldwurm S, et al. Striatal dopamine transporter binding in Parkinson’s disease associated with the LRRK2 Gly2019-Ser mutation. *Mov Disord* 2006;21:1144–1147.
33. Tashiro Y, Drake JM, Chakraborty S, Hattori T. Functional injury of cholinergic, GABAergic and dopaminergic systems in the basal ganglia of adult rat with kaolin-induced hydrocephalus. *Brain Res* 1997;770:45–52.
34. Hwang YS, Shim I, Chang JW. The behavioral change of locomotor activity in a kaolin-induced hydrocephalus rat model: evaluation of the effect on the dopaminergic system with progressive ventricle dilatation. *Neurosci Lett* 2009;462:198–202.
35. DeVito EE, Salmond CH, Owler BK, et al. Caudate structural abnormalities in idiopathic normal pressure hydrocephalus. *Acta Neurol Scand* 2007;116:328–332.
36. Keong NC, Pena A, Price SJ, et al. Diffusion tensor imaging profiles reveal specific neural tract distortion in normal pressure hydrocephalus. *PLoS One* 2017;12:e0181624.
37. Fasano A, Herman T, Tessitore A, et al. Neuroimaging of freezing of gait. *J Parkinsons Dis* 2015;5:241–254.
38. Bartels AL, de Jong BM, Giladi N, et al. Striatal dopa and glucose metabolism in PD patients with freezing of gait. *Mov Disord* 2006; 21:1326–1332.
39. Iacono RP, Tang ZS, Mazziotta JC, et al. Bilateral fetal grafts for Parkinson’s disease: 22 months’ results. *Stereotact Funct Neurosurg* 1992;58:84–87.
40. Lee CC, Lin SZ, Wang Y, et al. First human ventral mesencephalon and striatum cografing in a Parkinson patient. *Acta Neurochir Suppl* 2003;87:159–162.
41. Cabral D, Beach TG, Vedders L, et al. Frequency of Alzheimer’s disease pathology at autopsy in patients with clinical normal pressure hydrocephalus. *Alzheimers Dement* 2011;7:509–513.
42. Leinonen V, Koivisto AM, Savolainen S, et al. Post-mortem findings in 10 patients with presumed normal-pressure hydrocephalus and review of the literature. *Neuropathol Appl Neurobiol* 2012;38: 72–86.
43. Espay AJ, Da Prat GA, Dwivedi AK, et al. Deconstructing normal pressure hydrocephalus: Ventriculomegaly as early sign of neurodegeneration. *Ann Neurol* 2017;82:503–513.
44. Bräutigam K, Vakis A, Tsitsipanis C. Pathogenesis of idiopathic normal pressure hydrocephalus: a review of knowledge. *J Clin Neurosci* 2019;61:10–13.
45. Peterson KA, Mole TB, Keong NCH, et al. Structural correlates of cognitive impairment in normal pressure hydrocephalus. *Acta Neurol Scand* 2019;139:305–312.

SGML and CITI Use Only  
DO NOT PRINT

Author Roles

1 Research project: A. Conception, B. Organization, C. Execution; 2 Statistical Analysis: A. Design, B. Execution, C. Review and Critique; 3 Manuscript Preparation: A. Writing of the First Draft, B. Review and Critique.

N.G.P.: 1A, 1B, 2A, 2B, 3A

J.B.: 1C, 2A, 2B, 3A

M.T.: 1A, 1B, 1C, 2C, 3A

B.M.: 1C, 2C, 3B

R.Z.: 1C, 2C, 3B

I.B.: 1C, 2C, 3B

G.T.: 1C, 2C, 3B

R.C.: 2C, 3B

P.V.: 1C, 3B

I.U.I.: 2C, 3B

A.F.: 2C, 3B

C.P.: 1A, 1B, 1C, 2C, 3A

Full financial disclosure for all authors (for the preceding 12 months)

J.B. received a scholarship from the German Research Foundation (Deutsche Forschungsgemeinschaft [DFG] grant BR 6121/1-1). R.C. is part of Advisory Boards for AbbVie, UCB, and Zambon; he received honoraria from AbbVie, General Electric, Lundbeck, Lusofarmaco, UCB, and Zambon. I.U.I. received honoraria from Medtronic PLC as well as grants from DFG, Fondazione Grigioni, and Fresco Foundation. A.F. provided consultancies to Abbott, AbbVie, Boston Scientific, Chiesi Farmaceutici, Ipsen, Medtronic, Sunovion, and UCB; he is part of Advisory Boards for Abbott, AbbVie, Boston Scientific, and Ipsen; he received honoraria from Abbott, AbbVie, Boston Scientific, Ceregate, Chiesi Farmaceutici, Ipsen, Medtronic, Sunovion, and UCB as well as grants from AbbVie, Boston Scientific, Medtronic, University of Toronto, and Weston Foundation. C.P. provided consultancies to AbbVie, Boston Scientific, and Medtronic; he received honoraria from AbbVie, Boston Scientific, Medtronic, Lusofarmaco, and Zambon.